Simulation and optimization study on the methane combustion chamber

XING Jing-fang[1], QU Hong-qiang[1], HUI Ji[1], ZHENG Xue-jing[2], HU Fang-shu[2], WANG Ying-jie[2]

[1]Institute of Metrology of Hebei Province(Hebei Key Laboratory of Gas Metrology and Big Data Analysis(Preparation)), Shijiazhuang,050227, China
[2]School of Environmental Science and Engineering, Tianjin University, Tianjin 300350, China
E-mail : xjfhbjl@126.com

Abstract

This paper simulated and optimized the combustion chamber of the direct metering of the natural gas calorific value experimental platform. This material conducted a numerical simulation of methane combustion in the combustion chamber using ANSYS Fluent software, and the effects of different mixture inlet pipe length, combustion chamber diameter, and methane nozzle diameter on carbon monoxide emission concentration were studied. Aim to promote the complete combustion of methane, a more appropriate combustion chamber structure, and size were determined through carbon monoxide emission concentration. Through the comparison and analysis of the temperature field, velocity field, and concentration field of each component, it is suggested to set the length of the inlet pipe to 25 mm, and set the diameter of the combustion chamber and methane nozzle as 44 mm and 1.5 mm, respectively. After optimization, carbon monoxide emission concentration decreased from 27.9 PPM to 17.8 PPM, decreasing by 36.2%.

1. Introduction

Compared with coal and oil, natural gas contains almost no sulfur and dust after purification, and will not produce solid waste and excessive carbon dioxide after combustion. It has prominent advantages of low carbon and is a clean and low-carbon basic energy [1]. Figure. 1 shows that the global consumption of natural gas has been on the rise in recent decades.

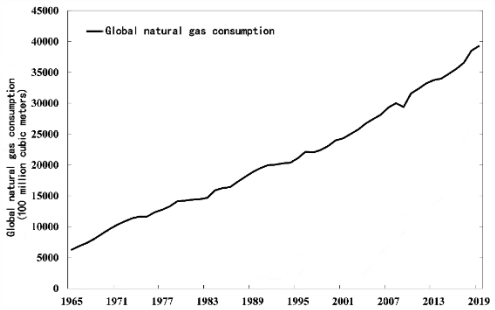

Figure 1: Global natural gas consumption.

In 2021, the global trade in liquefied natural gas reached 380 million tons, an increase of 6%. In the natural gas trade, metering methods mainly include volume metering, mass metering, and energy metering. Since the thermal energy of natural gas is the fundamental factor to judge its value, energy metering is more scientific and reasonable. At present, volume metering is widely used, while it will lead to unfair natural gas trade. Because the same volume of natural gas may have different components and calorific values due to different gas sources. Therefore, the adoption of volume metering is highly likely to cause commercial disputes or major economic losses. In addition, since the metering method adopted in some countries is different from that adopted in international trade, volume metering and energy metering will appear simultaneously in natural gas trade after the import of natural gas, resulting in settlement difficulties [3-4].To solve the above problems caused by the adoption of natural gas volume metering and speed up the technical level of natural gas energy metering in line with international standards, natural gas energy metering should be implemented as soon as possible.

According to the metering principle, the metering method of natural gas calorific value can be divided into the direct metering method and indirect metering method.

In the direct metering method, natural gas burns in excess air at a constant flow rate, and the heat released in the combustion process is transferred to the endothermic medium, causing the temperature rise of the endothermic medium, and the calorific value of natural gas is directly related to the temperature rise. It is mainly divided into the oxygen bomb metering method, catalytic combustion reaction method, and open flame combustion method [5]. The basic structure of the oxygen bomb calorimeter includes an oxygen bomb, calorimeter, and thermometer [6]. At present, only The National Institute of Metrology has carried out relevant research on the oxygen bomb calorimeter used to measure the calorific value of natural gas. Many foreign studies on oxygen bomb calorimeters focus on the micro oxygen bomb calorimeter for measuring the combustion heat of trace organic materials [7-12]. In a catalytic

combustion reaction, gas and air pass through a packed bed made of catalyst particles. In this process, the gas is oxidized and the heat released during the reaction causes the temperature of the packed bed to rise. Flame-releasing combustion method is to make the known mass gas sample in the combustion chamber for constant pressure combustion, the heat released in the combustion process is transferred to the heat absorption medium, and the heat absorption medium will have a certain temperature rise. By measuring the temperature rise, the heat capacity of the calorimetric device can be calculated to measure the heat of the gas sample.

Many studies have shown that among the above calorimeters, the isoperimetric calorimeter based on the fixed-mass open flame combustion method has the highest accuracy in measuring the calorific value of gas [13].

The indirect metering method is to analyze the components of natural gas through analytical technology. According to the calorific value of each component in natural gas in ISO 6976, the calorific value of the gas sample to be measured is calculated [14]. In the natural gas trade, the indirect metering method is widely used to measure the calorific value of samples while the direct metering method of calorific value is the basis of traceability, which can directly trace the calorific value of natural gas to the national combustion heat reference device. Meantime, it is also the basis of indirect metering of calorific value, and can also be used to test the accuracy of indirect metering results. Therefore, the direct measurement of calorific value is an important technology to realize the energy measurement of natural gas. It is necessary to establish a complete set of a direct measurement device to ensure the traceability of natural gas calorific value. And take it as the comparison and verification standard of indirect measurement traceability chain of calorific value to ensure the accuracy of energy measurement and valuation, so as to realize the accuracy and fairness of natural gas trade.

Accurate metering of gas calorific value is the foundation of realizing natural gas pricing according to the energy metering. As the main component of natural gas, accurate measurement of methane calorific value is the base of natural gas calorific value measuring. Therefore, from the perspective of reducing carbon monoxide emission concentration, this paper aims to promote the complete combustion of methane and optimize the combustion chamber part of the direct metering of the natural gas calorific value experimental platform. The structure of the experimental platform for direct calorific value measurement is shown in Figure 2. ANSYS Fluent software was used to optimize the simulation of the combustion chamber, and the influence of the structure and size of the mixed gas inlet pipe, the diameter of the combustor, and the diameter of the methane nozzle on the carbon monoxide emission concentration was analyzed. Through the carbon monoxide emission concentration to determine whether the result promoted the methane complete combustion or not. Therefore, the structure and size of the combustor that is more conducive to methane complete combustion were determined, which can provide reference and guidance for further realization of natural gas complete combustion.

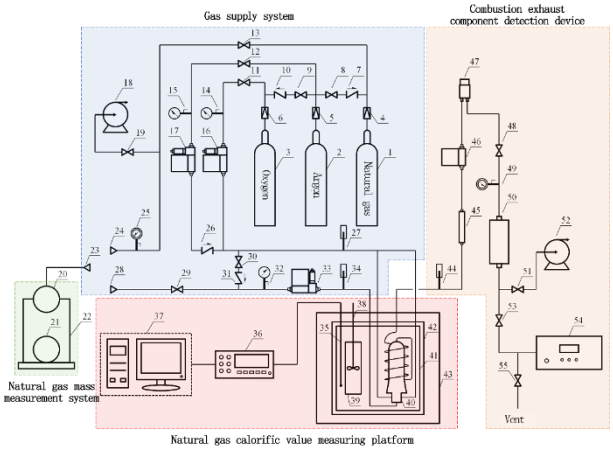

Figure 2: Schematic diagram of an experimental platform for the mea surement of methane calorific value

2 Mathematical models of the combustion chamber

2.1 Model simplification and assumptions

To accurately calculate the temperature field, velocity field, and concentration field of each component in the combustion chamber, improve the calculation efficiency and reduce the calculation time, the combustion situation in the combustion chamber is simplified and assumed as follows:

(1) The combustion chamber is in steady-state combustion;

(3) Combustion products are carbon monoxide, carbon dioxide, and water vapor;

(4) The water in the combustion product is gaseous.

2.2 Governing Equation

The methane combustion in the combustion chamber can be described by mass balance equation, component mass balance equation, momentum balance equation, energy balance equation, turbulence model, radiation model, and chemical reaction model, which are detailed as follow:

(1) Mass balance equation

$$\frac{\partial \rho}{\partial t} + div(\rho \vec{v}) = S_m \quad (1)$$

(2) Component mass balance equation

$$\frac{\partial (\rho C_A^*)}{\partial t} + div(\rho C_A^* \vec{v}) = div\left(Dgrad(\rho C_A^*)\right) + S_A \quad (2)$$

(3) Momentum balance equation

$$\frac{\partial (\rho \vec{v})}{\partial t} + div(\rho \vec{v} v_x) = div(\mu \cdot grad v_x) - \frac{\partial p}{\partial x} + F_x \quad (3)$$

$$\frac{\partial (\rho \vec{v})}{\partial t} + div\left(\rho \vec{v} v_y\right) = div\left(\mu \cdot grad v_y\right) - \frac{\partial p}{\partial x} + F_y \quad (4)$$

$$\frac{\partial(\rho\vec{v})}{\partial t} + div(\rho\vec{v}v_z) = div(\mu \cdot grad v_z) - \frac{\partial p}{\partial x} + F_z \quad (5)$$

(4) Energy balance equation

$$\frac{\partial(\rho T)}{\partial t} + div(\rho T\vec{v}) = div\left(\frac{\lambda}{c_p} grad T\right) + \frac{S_T}{c_p} \quad (6)$$

(5) Turbulence model

The Standard K -ε turbulence model is used to simulate methane combustion. Since its robustness, economy, and reasonable accuracy, this model has been widely used in practical engineering fluid calculation. The turbulent kinetic energy and its dissipation rate in the Standard K -ε model can be obtained from Equations (7) to (12).

$$\frac{\partial(\rho k)}{\partial t} + \frac{\partial(\rho k u_i)}{\partial x_i} = \frac{\partial}{\partial x_j}\left[\left(\mu + \frac{\mu_t}{\sigma_k}\right)\frac{\partial k}{\partial x_j}\right] + G_k + G_b - \rho\varepsilon - Y_M + S_k \quad (7)$$

$$\frac{\partial(\rho\varepsilon)}{\partial t} + \frac{\partial(\rho\varepsilon u_i)}{\partial x_i} = \frac{\partial}{\partial x_j}\left[\left(\mu + \frac{\mu_t}{\sigma_\varepsilon}\right)\frac{\partial \varepsilon}{\partial x_j}\right] + C_{1\varepsilon}\frac{\varepsilon}{k}(G_k + C_{3\varepsilon}G_b) - C_{2\varepsilon}\rho\frac{\varepsilon^2}{k} + S_\varepsilon \quad (8)$$

$$\mu_t = \rho C_\mu \frac{k^2}{\varepsilon} \quad (9)$$

$$G_k = -\rho\overline{u_i' u_j'}\frac{\partial u_j}{\partial x_i} \quad (10)$$

$$G_b = \beta g_i \frac{\mu_t}{Pr_t}\frac{\partial T}{\partial x_i} \quad (11)$$

$$C_{3\varepsilon} = tanh\left|\frac{v_y}{v_x}\right| \quad (12)$$

(6) Radiation model

The Discrete Ordinates (DO) radiation model, which covers the entire optical thickness range, is used to solve various problems such as face-to-face radiation to combustion radiation. The DO model regards the radiative transfer equation in the direction as a field equation, as shown in Equation (13).

$$\mathrm{div}(I(\vec{r},\vec{s})\vec{s}) + (a+\sigma_s)I(\vec{r},\vec{s}) = an_r^2\frac{\sigma T^4}{\pi} + \frac{\sigma_s}{4\pi}\int_0^{4\pi} I(\vec{r},\vec{s})\Phi(\vec{s},\vec{s}')d\Omega' \quad (13)$$

(7) Chemical reaction model

In the simulation, the methane two-step reaction mechanism is selected, and its chemical equation is shown in Equation (14). Component transport model, vortex dissipation model, and vortex dissipation conceptual model are used to simulate methane combustion.

$$\begin{cases} 2CH_4 + 3O_2 = 2CO + 4H_2O \\ 2CO + O_2 = 2CO_2 \end{cases} \quad (14)$$

In the component transport model, the mixing and transport of chemical components are simulated by solving the conservation equations describing the convection, diffusion, and reaction sources of each component. In the vortex dissipation model, it is assumed that the reaction rate is controlled by turbulence, and the influence of the chemical time scale is ignored to avoid complex chemical kinetics calculations. In the vortex dissipation conceptual model, the time scale of turbulence and dynamics is taken into account, so the turbulent flame contains detailed chemical dynamics, but it also causes an increase in computational cost [13].

In the simulation process, to combine the advantages of the vortex dissipation model and the vortex dissipation conceptual model, the vortex dissipation model was used to preliminarily simulate the combustion of methane firstly and obtained a more accurate temperature field. Then further simulated the detailed combustion conditions of methane by the vortex dissipation conceptual model.

2.3 Univalued condition

Geometric conditions are the shape and size of the wall surrounding the calculation area. For the calculation domain studied in this manuscript, including the combustion chamber, the local mixed gas inlet pipe connected to the combustion chamber, the exhaust pipe, and the methane inlet pipe that enters the combustion chamber. The geometric model and detailed size are shown in Figure 3.

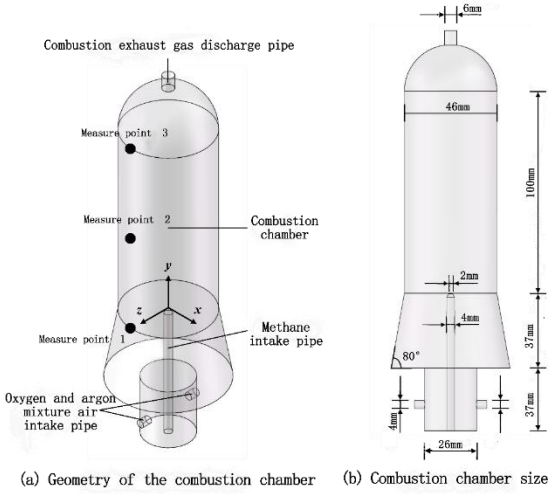

Figure 3: Combustor geometry model and dimensions

Physical conditions are physical characteristics of substances involved in flow and heat and mass transfer. For the methane combustion reaction studied in this paper, the substances involved include the mixture of all components in the combustion reaction (methane, oxygen, carbon dioxide, carbon monoxide, nitrogen) and quartz glass, the material of the combustion chamber, and each pipe. For the mixture, its related properties are determined by the chemical reaction model of methane combustion. For glass, detailed parameters given by the manufacturer of combustion chamber customization are used, as shown in Table 1.

Table 1: Physical properties of quartz glass

Parameter name	**Parameter value**
Density	2200 kg/m^3
Short term service temperature	1300 ℃
Long term service temperature	1100 ℃
Specific heat capacity	670 J/(kg·℃)
Thermal conductivity	1.4 W/(m·℃)
Refractive index	1.4585

Boundary conditions are to solve the variation rule of the variables on the boundary of the region. For the combustion chamber studied in this paper, it is necessary to set the boundary structure of methane inlet, mixed gas inlet, combustion exhausts outlet, and the

inner wall of the combustion chamber and each pipe. The boundary-setting of the combustion chamber is shown in Figure 4.

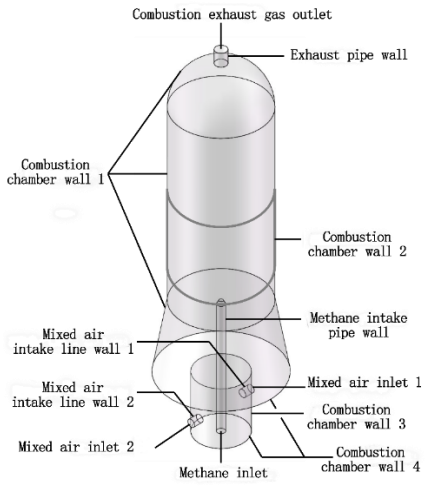

Figure 4: Combustion chamber boundary setting

(1) Methane inlet and mixture inlet
The boundary type of the methane inlet and the mixture inlet is set as the velocity inlet. During the experiment, the flow rate of methane was 70 SCCM, and the mixed flow rate of oxygen and argon was 360 SCCM, based on the set value of the flow rate of each gas and their densities under standard conditions and experimental conditions respectively. The calculated velocity of methane inlet and mixture inlet is 0.102 m/s and 0.263 m/s respectively. The temperature of the methane inlet and mixture inlet is set at 301.15K.

(2) Combustion exhausts outlet
The boundary type of combustion exhausts outlet is set as pressure outlet, and the gauge pressure at the outlet is set as 0 Pa.

(3) Combustion chamber and each pipe wall
The boundary type of the combustion chamber and each pipe wall is set as a wall. For the wall of the methane inlet pipe, the thermal boundary condition of the wall of the methane inlet pipe is set as Coupled since both the inner and outer sides of the methane inlet pipe are computational domains. For the combustion chamber wall, mixed air inlet pipe, and exhaust pipe wall, the third type of boundary conditions (except the methane inlet pipe wall) are adopted, and the heat transfer coefficient of the wall and the fluid temperature of the outside are required to be given. The wall heat transfer coefficient is divided into two cases for setting. One is the production of condensed water on the inner wall, that is, the combustion chamber wall 2 shown in Figure 3. Second, there is no condensation water on the inner wall, including all the other walls except the combustor wall 2. In the first case, the heat transfer coefficient is set at 55 W/(m2 ·℃)[14]. In the second case, the heat transfer coefficient can be calculated. Table 2 shows the calculation results of the heat transfer coefficient on each wall. For the external fluid temperature, set to 301.15K.

Table 2: Calculation results of heat transfer coefficient of each wall surface

The name of the wall	Heat transfer coefficient [W/(m^2 ·℃)]
Combustion chamber wall 1	11.29
Combustion chamber wall 3	11.26
Combustion chamber wall 4	11.31
Mixture air inlet wall 1/2	10.95
Exhaust pipe wall	11.17

3 Model Verification

To verify the accuracy and reliability of the simulation results, the combustion chamber was divided into 540,878 grids, and the simulation results were compared with the measured results. The comparison items included the temperature and carbon monoxide emission concentration of the three metering points, and the positions of the three metering points were shown in Figure 3(a). Table 3 shows the data comparison between simulation results and experimental results.

Table 3: Comparison between simulation results and experimental results

	The temperature at point 1 (℃)	**The temperature at point 2 (℃)**	**The temperature at point 3 (℃)**	**Carbon monoxide emission concentration (ppm)**
Experimental results	79.0	107.5	158.5	30
Simulation results	82.4	112.0	166.5	27.9
Absolute error	3.3	4.5	8.0	-2.1
Relative error(%)	4.2	4.2	5.0	-6.8

Based on the above error analysis of temperature and carbon monoxide emission concentration simulation results, it is considered that the number of grids of 540878 can meet the accuracy requirements of simulation.

4 Simulation results and analysis

4.1 Influence of mixture inlet pipe structure and length on carbon monoxide emission concentration
Figure. 5 shows the velocity distribution and oxygen molar concentration distribution at the x=0 section of the combustion chamber under the mixed air inlet pipe structure as shown in Figure. 3 (a). It can be seen that the mixture of oxygen and argon will diffuse immediately after entering the combustion chamber. When it diffuses to the methane nozzle, its velocity is close to zero, causing the low oxygen concentration near the methane nozzle. To avoid premature diffusion of the mixture of oxygen and argon and make the mixture further diffuse to the vicinity of the methane nozzle, the mixed air inlet pipe structure as shown in Figure. 6 is adopted to achieve the purpose of reducing

carbon monoxide emission concentration and making methane combustion more complete.

In addition, the inlet length of the mixed air inlet pipe will also affect the carbon monoxide emission concentration. The oxygen concentration near the methane nozzle rises less when the inlet length is too short. If the inlet length is too long, the temperature in the combustion area may decrease due to the oxygen not diffusing to the methane nozzle in time or diffusing unevenly near the methane nozzle, resulting in a poor combustion effect. For this reason, after improving the structure of the mixed air inlet pipe, the inlet lengths of different mixed air inlet pipes were studied. Table 4 shows the mean oxygen molarity of the methane nozzle cross-section, the highest temperature in the combustion chamber, and the carbon monoxide emission concentration under different inlet lengths of the mixed air inlet pipe.

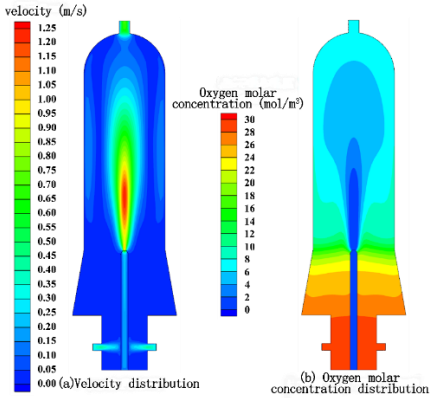

Figure 5: The distribution of velocity and oxygen molar concentration at the x=0 section of the combustion chamber under the original mixed air inlet pipe structure

Figure 6: Improved combustion chamber after mixed air inlet pipe

Table 4: Simulation results under different inlet lengths of mixed air

The length of the pass (mm)	Mean molarity of oxygen at the methane nozzle cross-section (mol/m^3)	Max temperature (℃)	Carbon monoxide emission concentration (ppm)
0 （Original）	16.14	1768.1	27.9
15	16.47	1770.7	27.1
25	16.55	1782.9	25.8
35	14.81	1768.2	28.7

As can be seen from Table 4, with the increase of the inlet length, the average oxygen molarity of the methane nozzle section and the maximum temperature in the combustion chamber after rising to decline. Therefore, the inlet length of the mixed air intake pipe is 25 mm. Under this inlet length, oxygen can effectively diffuse to the vicinity of the methane nozzle.

Figure. 7 shows the velocity distribution and oxygen molar concentration distribution in the combustion chamber after the inlet pipe of the mixed gas is improved and the inlet length is 25 mm.

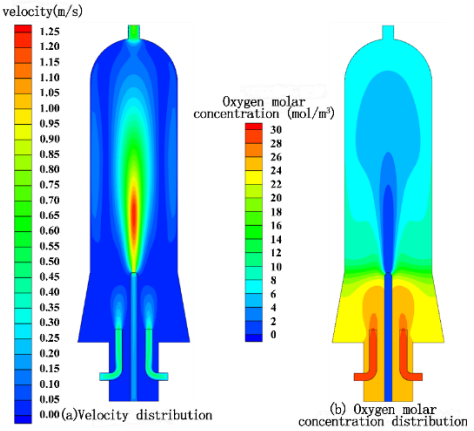

Figure 7: The velocity and oxygen molar concentration distribution of combustion chamber x=0 section when the inlet length of the mixed air inlet pipe is 25 mm

In conclusion, after improving the structure of the mixed air inlet pipe, the mixture of oxygen and argon further diffused to the vicinity of the methane nozzle, resulting in an increase in oxygen concentration and temperature in the combustion reaction area. In addition, when the inlet length of the mixture inlet pipe is set to 25 mm, a more significant effect is achieved in enhancing the complete combustion of methane, and the carbon monoxide emission concentration is reduced by 2.1 PPM compared with that of the original mixture inlet pipe.

4.2 Effect of combustor diameter on carbon monoxide emission concentration

In this section, to further increase oxygen concentration and achieve lower carbon monoxide emission concentration, the method of reducing the diameter of the combustion chamber is adopted. With the decrease of combustion chamber diameter, the increase of oxygen concentration helps to fully contact methane with oxygen, and the temperature in the combustion reaction area increases. However, at the same time, the gas flow rate in the combustion chamber will increase, resulting in the enhancement of heat dissipation near the flame. The temperature in this region will decrease, resulting in the deterioration of the combustion effect and the increase of the carbon monoxide emission concentration. Therefore, it is necessary to determine the appropriate combustion chamber diameter to ensure

the increase of oxygen concentration and avoid the adverse effect of the increase of gas flow rate on the reduction of carbon monoxide emission concentration.

Figure. 8 and Table 5 show the simulation results under different combustion chamber diameters. When the diameter of the combustion chamber is reduced from 46 mm to 44 mm, the molar concentration of oxygen near the methane nozzle and the mean molar concentration of oxygen in the cross-section of the methane nozzle both rise gradually, indicating that the increase of oxygen concentration promotes the combustion reaction between methane and oxygen. When the diameter of the combustion chamber is reduced from 44 mm to 42 mm, although the oxygen molar concentration near the methane nozzle and the average oxygen molar concentration of the methane nozzle cross-section are still rising, the continuous increase of the gas flow rate of the methane nozzle cross-section further strengthens the heat dissipation effect in the combustion area, resulting in a decrease of the temperature in the combustion chamber. It has the opposite effect on promoting the complete combustion of methane, increasing carbon monoxide emission concentration.

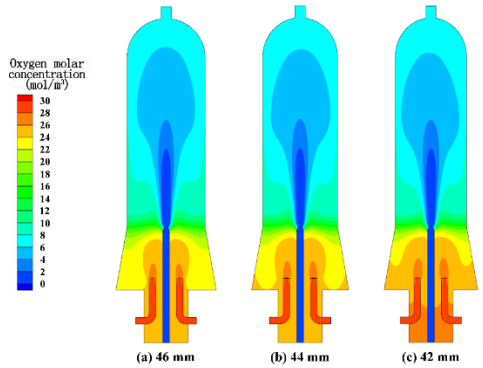

Figure 8: Oxygen molar concentration distribution of combustion chamber x=0 section under different combustion chamber diameters

Table 5: Simulation results under different combustion chamber diameters

Combustion chamber diameter (mm)	Mean molarity of oxygen at the methane nozzle cross-section (mol/m^3)	Air velocity at the methane nozzle cross-section (mm/s)	Highest temperature (℃)	Carbon monoxide emission concentration (ppm)
46（Original）	16.55	14.1	1782.9	25.8
44	16.78	14.8	1820.4	23.2
42	17.11	15.8	1810.2	25.1

Based on the analysis, at the same time as the oxygen concentration and gas flow rate increase, selecting 44 mm as chamber diameter can not only realize the oxygen concentration increase of methane combustion but also avoid the velocity increased inhibition of methane combustion. Finally, it can obtain a better combustion effect, to achieve lower carbon monoxide emission concentration.

4.3 Influence of methane nozzle diameter on carbon monoxide emission concentration

In sections 4.1 and 4.2, the combustion chamber is improved from the perspective of increasing oxygen concentration near the methane nozzle. In addition, increasing the concentration of methane itself also has a significant effect on promoting its complete combustion. From the perspective of increasing the concentration of methane, this section adopts the method of reducing the diameter of the methane nozzle. This method can make methane spews out from the nozzle in a more concentrated way, which is conducive to the centralized combustion of methane and the rise of the temperature in the combustion area, thus promoting the complete combustion of methane. However, with the decrease of the diameter of the methane nozzle, the gas velocity from the nozzle increases gradually, and the increase of the gas velocity will lead to the instability of the flame and make the combustion effect worse. In addition, the diameter of the methane nozzle is too small, which will increase the difficulty of processing. Therefore, it is necessary to determine the appropriate diameter of the methane nozzle to ensure the stability of flame and the feasibility of processing while increasing methane concentration.

Table 6 shows the simulation results under different diameters of methane nozzles. To show the comparison of methane concentrations at the same height after being pumped out of the nozzle under different diameters of methane nozzles, the molar concentration data of methane at the y=0 section, which is 0.2mm above the section where the methane nozzles are located, is adopted. It can be seen from the table that with the decrease of methane nozzle diameter, the average molar concentration of methane at the y=0 section decreases, the maximum temperature in the combustion chamber rises, and the emission concentration of carbon monoxide decreases.

Table 6: Simulation results under different methane nozzle diameters

Diameter of methane nozzle (mm)	Mean molar concentration of methane at y=0 cross-section (mol/m^3)	Highest temperature (℃)	Carbon monoxide emission concentration (ppm)
2（Original）	3.97×10^{-2}	1820.4	23.2
1.5	2.52×10^{-2}	1889.0	17.8
1	1.25×10^{-2}	2072.4	12.2

As for the change of temperature in the combustion chamber, as the diameter of the methane nozzle decreases, not only does the maximum temperature in the combustion chamber increase but also the high-temperature area in the combustion area gradually

increases, as shown in Figure. 9. The temperature rise is mainly caused by the concentrated combustion of methane. In the process of reducing the diameter of the methane nozzle, methane can be more concentrated out of the nozzle. Correspondingly, the combustion reaction is more concentrated and intense. At the same time, the temperature in the combustion area rises, and the rise of temperature is very beneficial to promoting the reaction of carbon monoxide and oxygen, to reduce the concentration of carbon monoxide emissions.

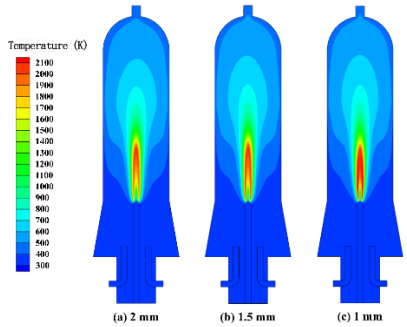

Figure 9: Temperature distribution of combustion chamber x=0 section under the different diameter of methane nozzle

Figure. 10 shows the velocity distribution of the combustion chamber x=0 section under different methane nozzle diameters. It can be seen that with the decrease of methane nozzle diameter, the combustion chamber velocity gradually increases. During the experiment, it was observed that flame stability and continuous combustion of methane could be achieved when the diameter of the nozzle was 2 mm. However, when the diameter of the nozzle decreased, flame jitter and unstable combustion might occur if the velocity increased too much. Figure. 11 further quantifies the velocity comparison of the central axis of the combustion chamber under different methane nozzle diameters. As can be seen from the Figureure, when the diameter of the nozzle is reduced to 1mm, the maximum velocity on the central axis is about 3.5 times that of the original diameter. Although the velocity decays quickly, the high-speed impact of about 3.5m /s will have a great impact on the stability of the flame.

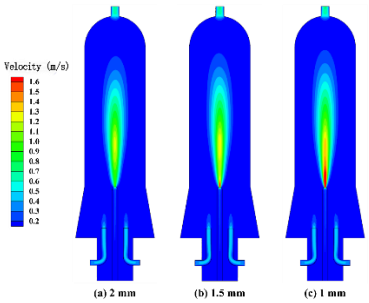

Figure 10: Velocity distribution of combustion chamber x=0 section under the different diameter of methane nozzle

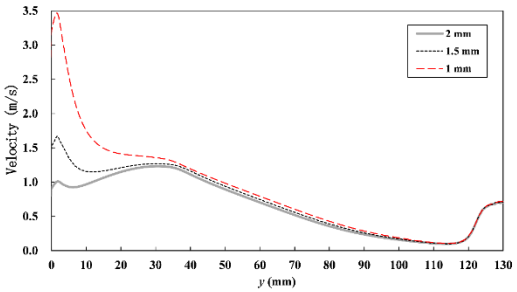

Figure 11: Velocity variation of the central axis of combustor under the different diameter of methane nozzle

In conclusion, when the diameter of the methane nozzle is reduced from 2 mm to 1.5 mm, methane can be sprayed out of the nozzle in a more concentrated way, increasing methane concentration. Accordingly, the methane combustion reaction is more concentrated and intense. Meanwhile, the temperature in the combustion area rises, which promotes the oxidation reaction of carbon monoxide. After the diameter of the methane nozzle was improved, carbon monoxide emission concentration was reduced from 23.2 PPM to 17.8 PPM.

5 Conclusions

In this paper, the simulation and optimization of the chamber were carried out. Firstly, the manuscript established the mathematical model of the combustion chamber, simplified and assumed the model, and gave the corresponding control equations and univalued conditions. The
control equations include the mass balance equation, component mass balance equation, momentum balance equation, energy balance equation, and the equations involved in the turbulence model, radiation model, and chemical reaction model. Univalued conditions include geometric conditions, physical conditions, and boundary conditions.

In this paper, methane was used as the gas sample, and simulations were conducted with the commercial software ANSYS Fluent. To determine the appropriate grid number and verify the simulation results are accurate and reliable, the simulation results were compared with the measured results. It is concluded that when the number of grids is 540878, the relative error between the simulated and measured temperature was about 5% and the relative error between the simulated and measured carbon monoxide emission concentration was -6.8 %. Under this number of grids, the simulation accuracy could meet the requirements, and would not occupy too much computing time.

Finally, this paper studies the different mixture structures and lengths, combustion chamber inlet pipe diameter, and nozzle diameter on the influence of the concentration of carbon monoxide emissions of methane. The carbon monoxide emission concentration reflected the completeness of methane combustion and determined the structure and length of the mixed gas inlet pipe, the diameter of the combustion chamber, and

the diameter of the methane nozzle that were conducive to promoting the complete combustion of methane, thus providing reference and guidance for the complete combustion of natural gas. After a comparative analysis of the temperature field, velocity field, and concentration field of each component in the combustion chamber, it was suggested to pass the mixed gas inlet pipe into the combustion chamber and made the inlet length 25 mm, the diameter of the combustion chamber 44 mm, and the diameter of the methane nozzle 1.5 mm. After optimization, carbon monoxide emission concentration decreased from 23.2 PPM to 17.8 PPM, a 36.2% reduction.

References

[1] Statistical Review of World Energy (69th Edition) [M/OL]. London: BP, 2020 [2021-10-18]. https://www.bp.com/content/dam/bp/business-sites/en/global/corporate/pdfs/energy-economics/statistical-review/bp-stats-review-2020-full-report.pdf.

[2] 周志斌，何润民，何春蕾，等. 中国实施天然气能量计量与计价的基础条件分析[J]. 国际石油经济，2011，19(10)：62-66+108.

[3] Peter Ulbig, Detlev Hoburg. Determination of the calorific value of natural gas by different methods [J]. Thermochimica Acta, 2002, 382(1-2): 27-35.

[4] ISO 6976 Natural Gas—Calculation of Calorific Values, Density, Relative Density and Wobbe Index from Composition, 2nd Edition, 1995 (corrected and reprinted in February 1996).

[5] L. I. Vorob'yov, T. G. Grishchenko, L. V. Dekusha. Bomb calorimeters for determination of the specific combustion heat of fuels [J]. Journal of Engineering Physics and Thermophysics, 1997, 70(5): 829-839.

[6] William S. Mcewan, Carl M. Anderson. Miniature bomb calorimeter for the determination of heats of combustion of samples of the order of 50 mg mass [J]. Review of Scientific Instruments, 1955, 26(3): 280-284.

[7] Minoru Sakiyama, Tetsu Kiyobayashi. Micro-bomb combustion calorimeter equipped with an electric heater for aiding complete combustion [J]. The Journal of Chemical Thermodynamics, 2000, 32(2): 269-279.

[8] Minas da Piedade, M. E. Oxygen bomb combustion calorimetry: principles and applications to organic and organometallic compounds. Energetics of Stable Molecules and Reactive Intermediates. NATO ASI Series C. Minas da Piedade, M. E.: editor. Kluwer: Dordrecht. 1999, 29–53.

[9] Aarón Rojas-Aguilar. An isoperibol micro-bomb combustion calorimeter for metering of the enthalpy of combustion. Application to the study of fullerene C60 [J]. The Journal of Chemical Thermodynamics, 2002, 34(10): 1729-1743.

[10] Aarón Rojas, Alejandro Valdés. An isoperibol micro-bomb calorimeter for metering of the enthalpy of combustion of organic compounds. Application to the study of succinic acid and acetanilide [J]. The Journal of Chemical Thermodynamics, 2003, 35(8): 1309-1319.

[11] Manuel A.V. Ribeiro da Silva, Geoffrey Pilcher, et al. Calibration and test of an aneroid mini-bomb combustion calorimeter [J]. The Journal of Chemical Thermodynamics, 2007, 39(5): 689-697.

[12] F. Haloua, B. Hay, J.-R. Filtz. New French reference calorimeter for gas calorific value meterings [J]. Journal of Thermal Analysis and Calorimetry, 2009, 97(2): 673-678.

[13] ISO 15112: 2018, Natural gas - Energy determination [S].

[14] Ansys Fluent Theory Guide [EB/OL]. Pennsylvania: ANSYS, Inc., 2021 [2021-10-18].https://ansyshelp.ansys.com/account/secured?returnurl=/View/Secured/corp/v212/en/flu_th/flu_th.html.